"NOTICE: this is the author's version of a work that was accepted for publication in International Journal of Impact Engineering. Changes resulting from the publishing process, such as peer review, editing, corrections, structural formatting, and other quality control mechanisms may not be reflected in this document. Changes may have been made to this work since it was submitted for publication. A definitive version was subsequently published in INTERNATIONAL JOURNAL OF IMPACT ENGINEERING, VOL 38, ISSUE 12, DECEMBER 2011, PAGES 1022-1032, DOI: 10.1016/j.ijimpeng.2011.08.005"

Ballistic performance of multi-layered metallic plates impacted by a 7.62-mm APM2 projectile

E.A. Flores-Johnson*, M. Saleh, L. Edwards

Institute of Materials Engineering, Australian Nuclear Science and Technology Organisation

Locked Bag 2001, Kirrawee DC, NSW, 2232 Australia

Abstract: This paper presents a numerical investigation of the ballistic performance of monolithic, double- and triple-layered metallic plates made of either steel or aluminium or a combination of these materials, impacted by a 7.62-mm APM2 projectile in the velocity range of 775-950 m/s. Numerical models were developed using the explicit finite element code LS-DYNA. It was found that monolithic plates have a better ballistic performance than that of multi-layered plates made of the same material. This effect diminishes with impact velocity. It was also found that double-layered plates with a thin front plate of aluminium and thick back steel plate exhibit greater resistance than multi-layered steel plates with similar areal density. These predictions indicate multi-layered targets using different metallic materials should be investigated for improved ballistic performance and weight-savings.

Keywords: Ballistic resistance; 7.62-mm APM2 projectile; multi-layered plates; numerical simulation.

*Corresponding author. Tel.: +61 2 9717 7348, Fax: +61 2 9717 9225, Email: efj@ansto.gov.au

1 INTRODUCTION

In recent years, the ongoing threat of ammunition and explosively-formed projectiles to civil and military structures has increased the need to optimise protective structures. Armoured shields normally consist of a monolithic high-strength metallic plate; however, multi-layered plate configurations are often used because armour materials are not always manufactured to the required thickness, and multiple layers are necessary to fabricate shields that meet design specifications [1]. Although there are a number of studies dealing with the ballistic behaviour of multi-layered plates, their scope is limited when compared to studies of monolithic plates [2-4]. Moreover, the study of multi-layered plates remains an open research topic since conclusive results of its effectiveness have not been obtained to date, as is remarked in recent investigations [3-4].

A numerical study conducted by Zukas and Scheffler [1] shows that 31.8 mm thick monolithic steel targets exhibit greater resistance than that of multi-layered targets with equal thickness when impacted by 65-mm long hemi-spherical nosed rods with a diameter of 13 mm and an initial velocity of 1164 m/s. They found that the weakening of the multi-layered configuration is due to the reduction of bending stiffness in the structure. They also found that the reduction of resistance in multi-layered targets becomes more apparent when the number of plates is increased while keeping the total thickness constant [1], which has also been observed experimentally [5-6]. Almohandes et al. [5] reported that monolithic steel plates are more effective than multi-layered plates of the same total thickness when impacted by a 7.62-mm projectile with an initial velocity of 826 m/s.

An investigation conducted by Dey et al. [2] on the ballistic resistance of Weldox 700E steel in the sub-ordnance velocity range shows that 12 mm monolithic plate has better ballistic performance against ogival projectiles when compared with double-layered plates with same thickness, while the opposite effect is observed when blunt projectiles are used. Borvik et al. [7] studied experimentally the same plate configurations using Weldox 700E steel against 7.62-mm APM2 projectiles. They found that the ballistic limit velocities of monolithic and double-layered plates were identical. However, 12 mm monolithic plate presented a slightly better performance for striking velocities above 850 m/s. A recent investigation by Teng et al. [3, 8] on the ballistic performance of monolithic and double-layered steel plates showed that the ballistic resistance depends on several factors, including projectile nose shape, projectile mass, impact velocity, configuration of the plates and material properties. Corran et al. [9] found that the projectile nose shape and hardness are very important to consider because the failure mechanisms involved in the penetration process and consequently the ballistic performance are dependent upon these factors. The above references show that the penetration process of multi-layered plates is a complex problem, which has not been fully understood. For design purposes, several of the aforementioned factors should be considered to obtain optimum protective structures.

Selection of materials for armour against ballistic threats is crucial not only for the protection effectiveness but also for weight reduction, which is very important from a design point of view, particularly in aircraft and automotive structures; however, the choice of armour would depend on several factors including price, design, specific application, ballistic performance, maintenance and weight [6]. Although high-strength steels are the primary candidate material for protective structures, engineering aluminium alloys such as Al 7075 and 7017 may be attractive candidates for armour applications due to their excellent strength-to-density ratio [10]. Although there are some experimental studies of the ballistic behaviour of engineering aluminium alloys [11-14], they are limited and few numerical simulations have been performed to further understand these results.

Numerical simulations to predict the performance of multi-layered plates have been used by several authors. Borvik et al. [7] used Lagrangian LS-DYNA simulations to model the impact of a 7.62-mm APM2 projectile on double-layered steel targets assuming axisymmetric conditions. They reported that good agreement between simulations and experiments was observed. Dey et al. [2] also used axisymmetric Langrangian simulations in LS-DYNA to predict the behaviour of double-layered Weldox 700E plates impacted by an ogival projectile. They reported that good agreement was observed between numerical simulations and experimental results. Borvik et al. [11] reported impact simulations of an ogival projectile on Al 7075-T651 monolithic plate using both axisymmetric and solid formulations. They found that both methods gave an overestimation of 30% of the ballistic limit, which was explained by the fact that the numerical simulations were not able to fully capture the brittle fracture behaviour of the target and the extensive fragmentation observed experimentally; however, fractures modes in the simulation were similar to those observed in the experiments. These studies show that numerical simulations can be used as a reliable tool to understand the ballistic behaviour of multi-layered plates.

As aforementioned, there are some studies dealing with the modelling of impact on double-layered plates; however, numerical predictions of the ballistic performance of multi-layered plates made with layers of different materials have not been studied in detail. In this paper, this problem is addressed by presenting numerical simulations dealing with the ballistic performance of monolithic and multi-layered targets made with either steel or aluminium or a combination of these materials impacted by a 7.62-mm APM2 projectile in the velocity range of 775-950 m/s using the explicit finite element code LS-DYNA [15]. An extensive and systematic parametric study is performed, as an equivalent experimental study would be very costly. The problem description and validation of the numerical models are described in Section 2. Numerical results are presented and discussed in Section 3 followed by conclusions.

2 PROBLEM DESCRIPTION AND MODEL VALIDATION

2.1 Problem description

The purpose of the present study is to investigate the effect of multi-layered armour plates with different configurations, thicknesses and material properties on the ballistic performance of the structure. A 7.62-mm APM2 projectile, the geometry of which is shown in Fig. 1, was used with initial impact velocities in the range of 775-950 m/s. Initial velocities were chosen according to NATO STANAG 4569 ballistic protection level 3 (930±20 m/s) [16]; however, lower initial impact velocities were also used to obtain the ballistic limit of the targets. Two materials were used for the target plates: Weldox 700E and Al 7075-T651.

Numerical simulations were carried out using the LS-DYNA finite element (FE) code [15]. The problem was considered to be symmetric, such that a half-model could be constructed to save computational expense, as shown in Fig. 1. The problem may be further simplified by assuming axisymmetry; however, a 3-D half-model would capture some realistic physical characteristics of the impact (e.g. bullet rotation) not considered in an axisymmetric model, without compromising computational resources. The mesh comprised 8-node brick elements with reduced integration and stiffness-based hourglass control with exact volume integration. The element size in the impact region was $0.33\times0.33\times0.33$ mm^3. It was demonstrated in previous work [17] that numerical simulations of the penetration resistance of double-layered steel plates impacted by a 7.62-mm APM2 projectile using this element size ($0.33\times0.33\times0.33$ mm^3) can produce good results. A limited mesh sensitivity analysis is also presented in Section 2.2. Contact between the different parts of the

model was modelled using an eroding single surface segment-based formulation [15]. No gap between layered plates was considered, and only contact as described before was defined between plates.

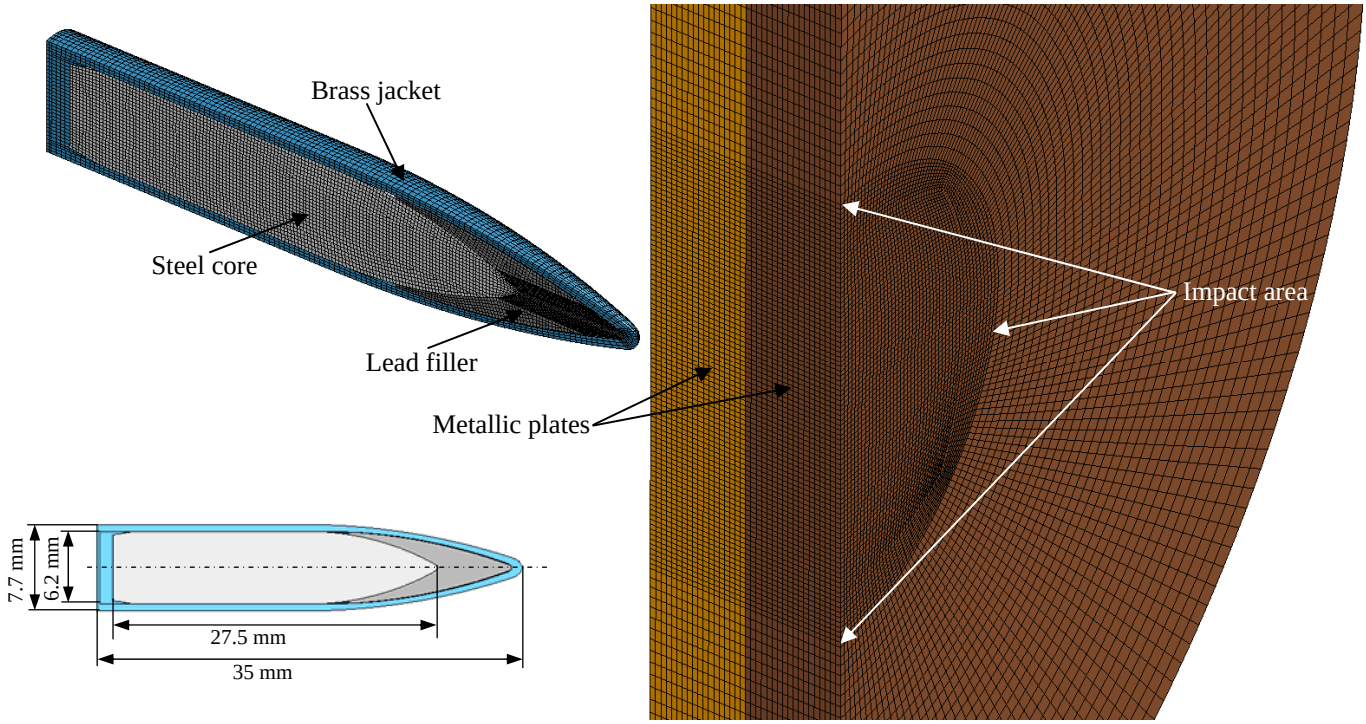

Figure 1 Finite element mesh of a 7.62-mm APM2 projectile impacting a metallic target.

The 7.62-mm APM2 projectile was modelled as three independent parts: Brass jacket, steel core, and lead filler (Fig. 1). The geometrical details of the 7.62-mm APM2 projectile are shown in Fig. 1. The total number of elements of the projectile was 48216.

The target was modelled as a 100-mm diameter circular plate. The impact region was considered to be a 30-mm diameter cylindrical-shaped zone at the centre of the plate (Fig. 1). Outside the impact region, the mesh coarsens radially towards the edge of the plate, while keeping same element thickness in the impact direction. The target plates were fully clamped at the edge boundaries. The total number of elements for a 12-mm thick plate was 318240. The number of elements increased up to 530400 for a 40-mm thick plate. The target configurations used in this study are shown in Table 1. Eight different total thicknesses T (12, 14, 16, 18, 20, 30, 36 and 40 mm) were considered to cover the range between the thinner target (12 mm for Weldox 700E) and thicker target (40 mm for Al 7075-T651) found in literature to validate the model. Five different configurations: monolithic, double-layered, triple-layered, double-layered mixed and triple-layered mixed were considered. Initial impact velocities in the range of 775-950 m/s were used in the simulations, giving the 97 different cases that are summarized in Table 1. The letters used in the target codes (Table 1) represent the layering configurations and the materials: M, monolithic; D, double; T, triple; DM, double-mixed; TM, triple-mixed, W, Weldox 700E; A, Al 7075-T651; while the numbers (12, 14, 16, 18, 20, 30, 36, 40) represent the total thickness of the targets. Simulation time for 12 mm thick plate using a 8-CPU SUN workstation with 42 gigabytes of RAM, varied from an hour for an initial velocity of 920 m/s to 6 hours for an initial velocity of 800 m/s. Simulation time increased for thicker plates up to 36 hours approximately for 40 mm thick plates and initial velocity of 800 m/s.

Table 1 Target plates configurations.

Configuration	Geometry	Code	Total thickness T (mm)	Layers	Areal density ρ_A (kg/m^2)	Initial impact velocity (m/s)
Monolithic	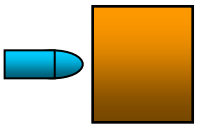	M12W, M12A	12	1×12 mm steel, 1×12 mm aluminium	94.2, 32.4	800, 950
		M14W	14	1×14 mm steel	109.9	800, 950
		M16W	16	1×16 mm steel	125.6	800, 810, 820, 850, 900, 950
		M18W	18	1×18 mm steel	141.3	800, 950
		M20W, M20A	20	1×20 mm steel, 1×20 mm aluminium	150, 54	800, 950
		M30A	30	1×30 mm aluminium	81	800, 950
		M36A	36	1×36 mm aluminium	97.2	800, 950
		M40A	40	1×40 mm aluminium	108	800, 950
Double-layered	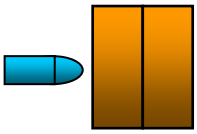	D12W, D12A	12	2×6 mm steel, 2×6 mm aluminium	94.2, 32.4	800, 950
		D14W	14	2×7 mm steel	109.9	800, 950
		D16W	16	2×8 mm steel	125.6	800, 810, 820, 850, 900, 950
		D18W	18	2×9 mm steel	141.3	800, 950
		D20W, D20A	20	2×10 mm steel, 2×10 mm aluminium	150, 54	800, 950
		D30A	30	2×15 mm aluminium	81	800, 950
		D36A	36	2×18 mm aluminium	97.2	800, 950
		D40A	40	2×20 mm aluminium	108	800, 950
Triple-Layered	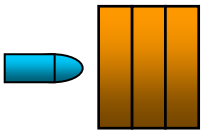	T12W, T12A	12	3×4 mm steel, 3×4 mm aluminium	94.2, 32.4	800, 950
		T14W	14	3×4.66 mm steel	109.9	800, 950
		T16W	16	3×5.33 mm steel	125.6	775, 780, 790, 800, 810, 820, 850, 900, 950
		T18W	18	3×6 mm steel	141.3	800, 950
		T20W, T20A	20	3×6.66 mm steel, 3×6.66 mm aluminium	150, 54	800, 950
		T30A	30	3×10 mm aluminium	81	800, 950
		T36A	36	3×12 mm aluminium	97.2	800, 950
		T40A	40	3×13.33 mm aluminium	108	800, 950
Triple-layered Mixed	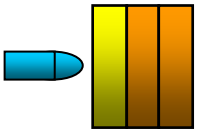	TM20AWW	20	1×6.66 mm aluminium+1×6.66 mm steel+1×6.66 mm steel		795, 800, 810, 820, 850, 900, 950
	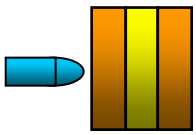	TM20WAW	20	1×6.66 mm steel+1×6.66 mm aluminium+1×6.66 mm steel	122.7	810
	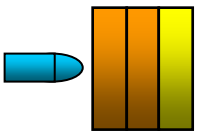	TM20WWA	20	1×6.66 mm steel+1×6.66 mm steel+1×6.66 mm aluminium		810
Double-layered Mixed	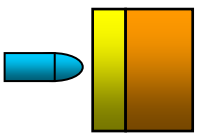	DM20AW	20	1×6.66 mm aluminium+1×13.33 mm steel		810, 815, 820, 850, 900, 950
	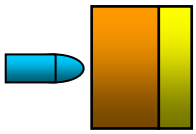	DM20WA	20	1×13.33 mm steel +1×6.66 mm aluminium	122.7	790, 800, 810, 820, 850, 900, 950

Both projectile and targets were modelled using a modified version of the well-known Johnson-Cook constitutive material model implemented in LS-DYNA (Material model 107) [15, 18-19]. This phenomenological model is expressed as [18],

$$\sigma_{eq} = (A + B\varepsilon_{eq}^{n})(1 + \dot{\varepsilon}_{eq}^{*})^{C}(1 - T^{*m}) \quad (1)$$

where σ_{eq} is the equivalent stress, ε_{eq} is the equivalent plastic strain, *A*, *B*, *n*, *C* and *m* are materials constants and $\dot{\varepsilon}_{eq}^{*} = \dot{\varepsilon}_{eq} / \dot{\varepsilon}_{0}$ is the dimensionless strain rate where $\dot{\varepsilon}_{eq}$ and $\dot{\varepsilon}_{0}$ are the strain rate and a user-defined strain rate, respectively. The homologous temperature is given as $T^{*} = (T - T_r)/(T_m - T_r)$, where *T* is the absolute temperature, T_r is the room temperature and T_m is the melting temperature. The temperature increment due to adiabatic heating is calculated as,

$$\Delta T = \int_{0}^{\varepsilon_{eq}} \chi \frac{\sigma_{eq} \mathrm{d}\varepsilon_{eq}}{\rho C_P} \quad (2)$$

where ρ is the material density, C_P is the specific heat and χ is the Taylor-Quinney coefficient that gives the proportion of work converted into heat [7].

The Cockcroft-Latham fracture criterion [20] which is implemented in Material model 107, was used to model failure. This criterion is expressed as,

$$W = \int_{0}^{\varepsilon_{eq}} \langle \sigma_1 \rangle \mathrm{d}\varepsilon_{eq} \leq W_{cr} \quad (3)$$

where *W* is the plastic work per unit volume and W_{cr} is critical value of *W* which can be determined from uniaxial tensile test, σ_1 is the major principal stress, $\langle\sigma_1\rangle=\sigma_1$ when $\sigma_1 \geq 0$ and $\langle\sigma_1\rangle=0$ when $\sigma_1<0$. Additionally, an element deletion criterion when the temperature of the element is equal to 90% of the melting temperature (Table 2) was used [7]. The modified Johnson-Cook material model has successfully been used to model impact on steel [2, 7, 21-22] and aluminium targets [11, 23-25]. Material model parameters used in the simulations are shown in Table 2 [7, 11].

2.2 Validation of the numerical model

Numerical models were validated against available experimental data of Weldox 700E and Al 7075-T651. Experimental results of the ballistic impact of 1x12 mm, 2x6 mm and 2x6 mm+30 mm air plates of Weldox 700E [7], and 1x20 mm and 2x20mm plates of Al 7075-T651 [12] are compared with numerical simulations in Fig. 2. The solid lines represent fits to the data of the Retch-Ipson model used to predict the residual velocity V_r [26],

$$V_r = a(V_i^{P} - V_{bl}^{P})^{1/P} \quad (4)$$

where *a* and P are empirical constants used to best fit the data and V_{bl} is the ballistic limit. It is noted that the original Recht-Ipson model with $a = m_p/(m_p + m_{pl})$ and P=2 [26-27] (where m_p and m_{pl} are the mass of the projectile and plug, respectively) is only applicable if the plastic deformation of the projectile is negligible [7]. It was observed experimentally that the perforation process of Weldox 700E and Al 7075-T651 plates does not involve any significant plugging when penetrated by 7.62-mm APM2 projectiles [7, 12]; therefore, *a*=1 and only P was fitted to the data. Fitted values of Recht-Ipson constants used in Eq. (4) are shown in Fig. 2; for the experimental data, these values were taken from [7, 12]. The ballistic limit was also obtained numerically by

fitting of the Retch-Ipson model (Eq. (4)) to the numerical results using at least six data points. The method of least squares was used to obtain the best fit of P and V_{bl} [28]; these values are shown in Fig. 2. It is noted that although P was fitted to both the experimental and numerical data, the values of P are very close to the value given in the analytical solution (P=2).

Table 2 Material properties and Modified Johnson-Cook model parameters.

Material properties	Weldox 700E [7]	Al 7075-T651 [11]	Steel core [7]	Lead cap [7]	Brass jacket [7]
Density ρ (kg/m^3)	7850	2700	7850	10660	8520
Young's modulus E (GPa)	210	70	210	1	115
Poisson's ratio ν	0.33	0.3	0.33	0.42	0.31
Taylor-Quinney coefficient χ	0.9	0.9	0.9	0.9	0.9
Specific heat C_p (J/kgK)	452	910	452	124	385
Expansion coefficient α (/K)	$1.2\text{x}10^{-5}$	$2.3\text{x}10^{-5}$	$1.2\text{x}10^{-5}$	$2.9\text{x}10^{-5}$	$1.9\text{x}10^{-5}$
Strain hardening					
A (MPa)	819	520	1200	24	206
B (MPa)	308	477	50000	300	505
N	0.64	0.52	1	1	0.42
Strain rate hardening					
Reference strain rate $\dot{\varepsilon}_0$ (s^{-1})	$5\text{x}10^{-4}$	$5\text{x}10^{-4}$	$5\text{x}10^{-4}$	$5\text{x}10^{-4}$	$5\text{x}10^{-4}$
C	0.0098	0.001	0	0.1	0.01
Temperature softening					
Reference temperature T_r (K)	293	293	293	293	293
Melting temperature T_m (K)	1800	893	1800	760	1189
m	1	1	1	1	1.68
Cockcroft and Latham failure criterion					
W_{cr} (MPa)	1486	106	-	175	914

Good agreement between experiment and simulation is observed. For Weldox 700E conservative results are obtained with approximately 4% overestimation of the ballistic limit. For Al 7075-T651 a slight underestimation of 1.2% is observed for 2x20 mm plates. For 1x20 mm Al 7075-T651 plate, conservative results are obtained with an overestimation of approximately 11% of the ballistic limit. These over and underestimations may attributed to the anisotropy and thickness dependency of the mechanical properties of Al 7075-T651 [10-11], which were not considered; however, the difference between predictions and experimental results are acceptable considering the complexity of the problem and the limitations of the constitutive relation and fracture criterion.

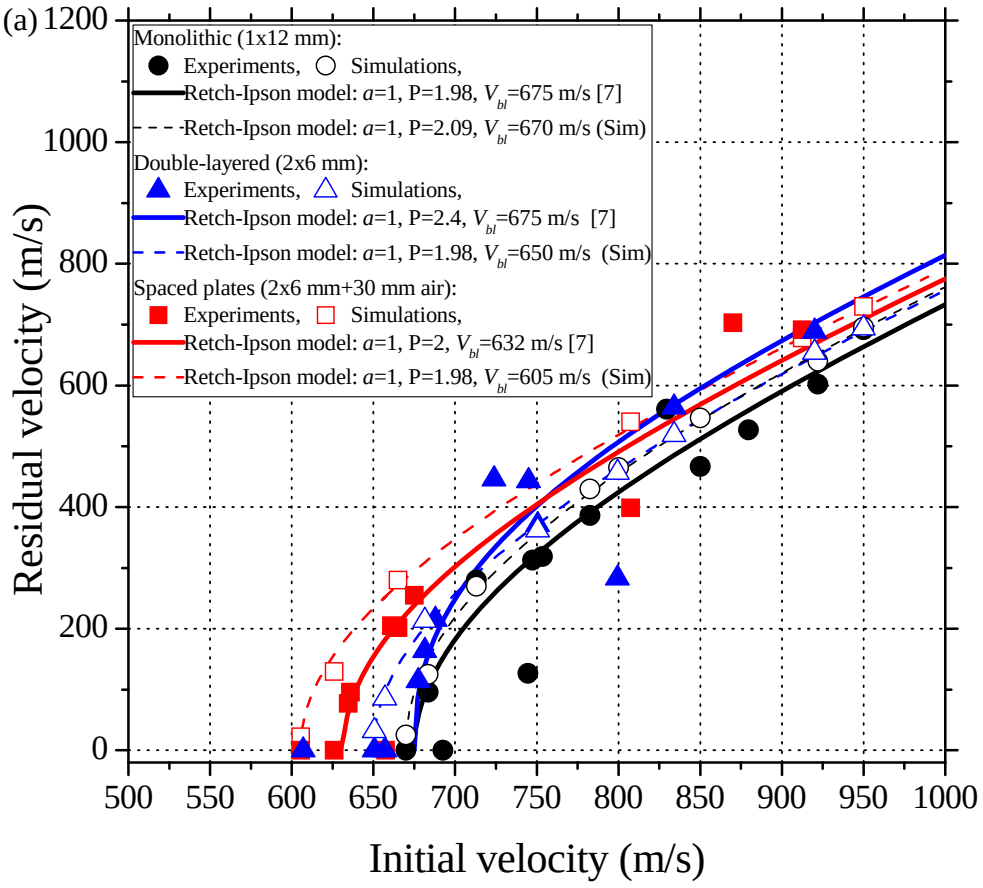

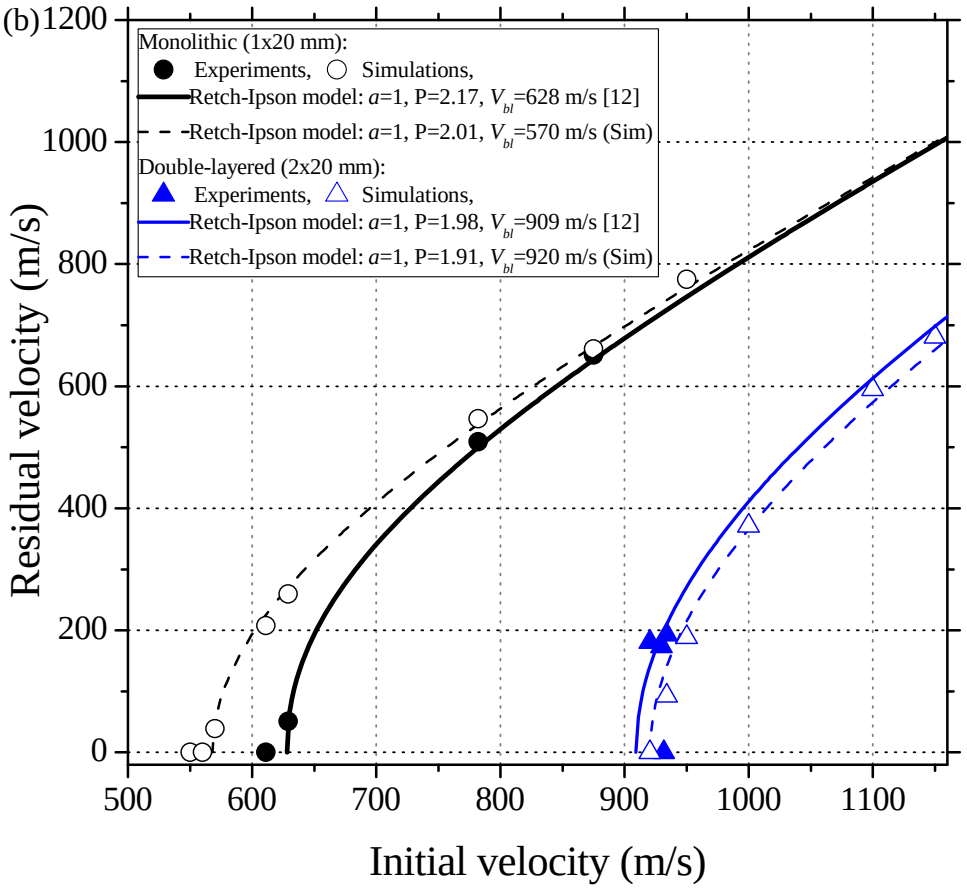

Figure 2 Comparison between experimental and predicted residual velocities for a) Weldox 700E [7] and b) Al 7075-T651 [12].

Figure 3 shows a series of model results depicting the penetration process of 2x6 mm double-layered Weldox 700E steel plates impacted by a 7.62-mm APM2 projectile with an initial impact velocity of 679 m/s. It can be seen that some of the physical behaviour observed during the penetration process of high strength steel targets [7] are well captured in the numerical simulation, such as stripping of the brass jacket and lead filler, dent on the side of the impact, and erosion and yawing of the bullet. Figure 3(f) shows the plates after all the projectile components have been removed to show the dent caused by the brass jacket. Figure 4 shows the predicted perforation process of 2x20 mm Al 7075-T651 plates impacted by a 7.62-mm APM2 projectile at 934 m/s. It can be observed that some of the physical characteristics observed experimentally in the penetration process of Al 7075-T651 plates by Forrestal et al. [12] are reproduced by the numerical model. For example, a complete stripping of brass jacket and lead cap from the steel core of the projectile is captured. The brittle failure reported in [12] was partially captured in the numerical simulations (spalling and fragmentation were observed in the target back face).

A limited mesh sensitivity analysis was carried out. Monolithic (1x12mm) and double-layered (2x6mm) Weldox 700E configurations and monolithic (1x20mm) Al 7075-T651 plate were impacted by a 7.62-mm APM2 projectile at 800 m/s. Three different element sizes were used in the impact region: 0.25×0.25×0.25 mm^3 (fine mesh), 0.33×0.33×0.33 mm^3 (intermediate mesh) and 0.4×0.4×0.4 mm^3 (coarse mesh), resulting in 48, 36 and 30 through-thickness elements for the Weldox 700E configurations, respectively, and 80, 60 and 50 through-thickness elements for the Al 7075-T651 configuration, respectively. The CPU-time was increased by factors of 1.6 and 3.5 for the intermediate and fine meshes, respectively, when compared to the coarse mesh. Figure 5 shows the projectile residual velocity predicted using different numbers of through-thickness elements. It can be seen that for Al 7075-T651 there is no significant difference in the predicted residual velocity between the intermediate mesh and the fine mesh (less than 0.6%), which agrees with the results reported by Borvik et al. [10]. For Weldox 700E, the differences between the results from the intermediate and fine meshes are 2.6 and 3.9% for the monolithic plate and double-layered plates, respectively. While using a fine mesh may increase model accuracy, an intermediate mesh (0.33×0.33×0.33 mm^3) is used in this work to increase computational efficiency due to the limitation of computational resources.

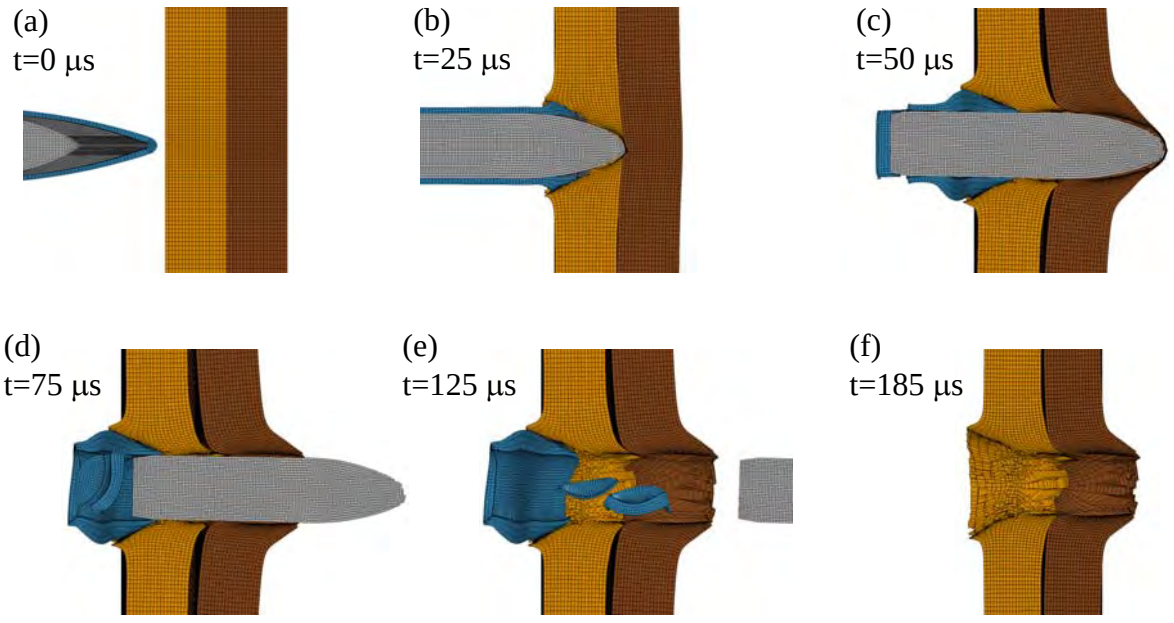

Figure 3 Penetration process of double-layered Weldox 700E steel plates impacted by a 7.62-mm APM2 projectile at 679 m/s.

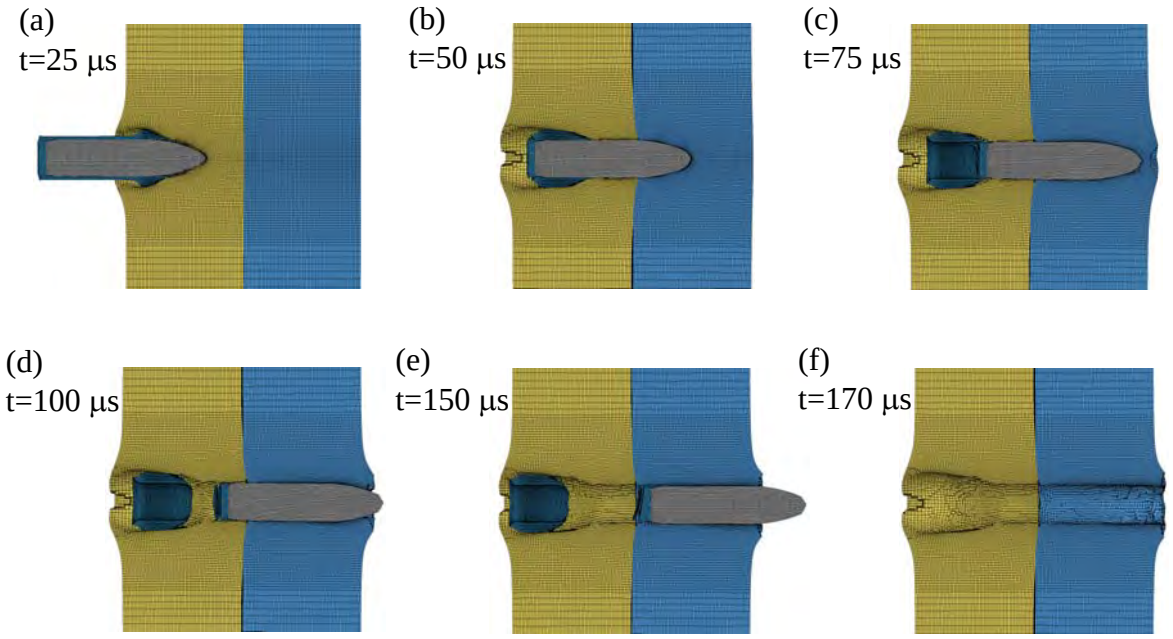

Figure 4 Penetration process of double-layered Al 7075-T651 plates impacted by a 7.62-mm APM2 projectile at 934 m/s.

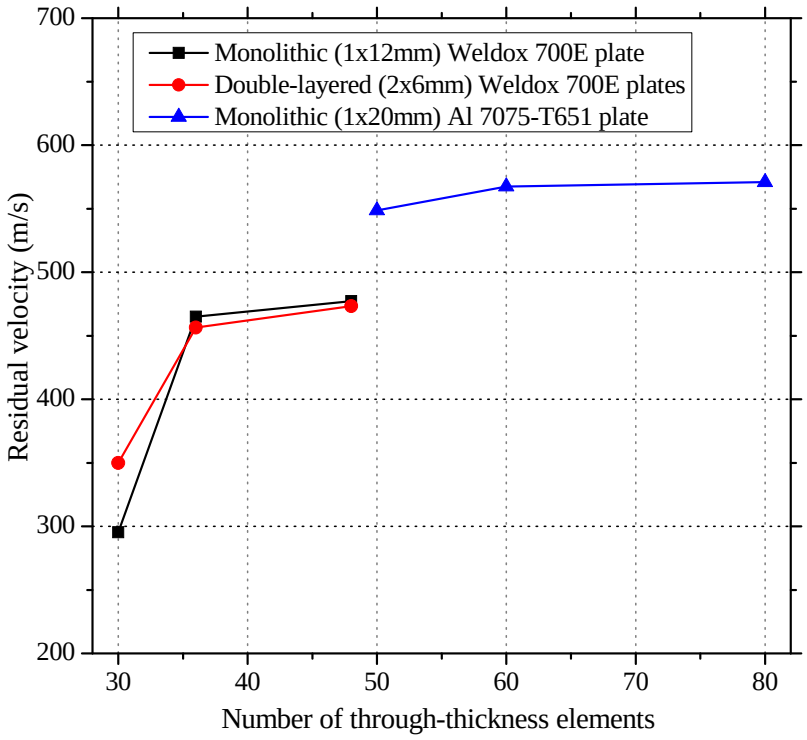

Figure 5 Predicted projectile residual velocities using different numbers of through-thickness elements for monolithic (1x12mm) and double-layered (2x6mm) Weldox 700E configurations and monolithic (1x20mm) Al 7075-T651 plate.

3 NUMERICAL SIMULATION RESULTS AND DISCUSSION

3.1 Effect of multi-layered configuration

Figure 6(a) shows the residual velocity V_r versus areal density for two initial impact velocities (800 and 950 m/s) and various multi-layered configurations of Weldox 700E steel plates (Table 1). Areal density ρ_A represents the mass per unit area of a multi-layered configuration of n plates and is defined as,

$$\rho_A = \sum_{i=1}^{n} \rho_i h_i \qquad (5)$$

where ρ_i and h_i are the density and thickness of the i^{th}-plate, respectively.

Figure 6(a) shows that V_r decreases with the increase of ρ_A as expected due to the increase of energy absorption capability in thicker targets. For V_i = 950 m/s, although the target performance decreases with an increase of the number of layers, the difference between monolithic and multi-layered plates is not significant. For V_i=800 m/s however this effect is more pronounced, which has also been observed by Almohandes et al. [5] who found that the difference in effectiveness between monolithic and multi-layered steel plates seems to diminish with impact velocity.

Figure 6(b) shows V_r versus ρ_A for various multi-layered configurations of Al 7075-T651 plates (Table 1) and V_i=800 and 950 m/s. As expected, V_r decreases with the increase of ρ_A due to the increase of target thickness. It can also be seen that the residual velocity of double- and triple-layered plates is similar to that of the monolithic plate when ρ_A<60 kg/m^2. However, for ρ_A>80 kg/m^2, the ballistic resistance of the monolithic plate is higher than that of multi-layered plates. This effect is more pronounced for V_i =800 m/s and total thicknesses of 36 and 40 mm. It is possible that this effect is due to an over-prediction of the monolithic plate stiffness; however, experimental data may be necessary to validate the accuracy of the predictions when ρ_A>80 kg/m^2.

Figure 7 shows perforation and interaction of plates of M12W, D12W, T12W, M16W, D16W, T16W, M12A, D12A, T12A, M20A, D20A and T20A configurations at t=0.07 ms, and initial velocities of V_i=800 and 950 m/s. It can be seen that monolithic plates exhibit greater bending resistance than double- and triple-layered configurations, while double-layered plates exhibit greater bending resistance than triple-layered plates.

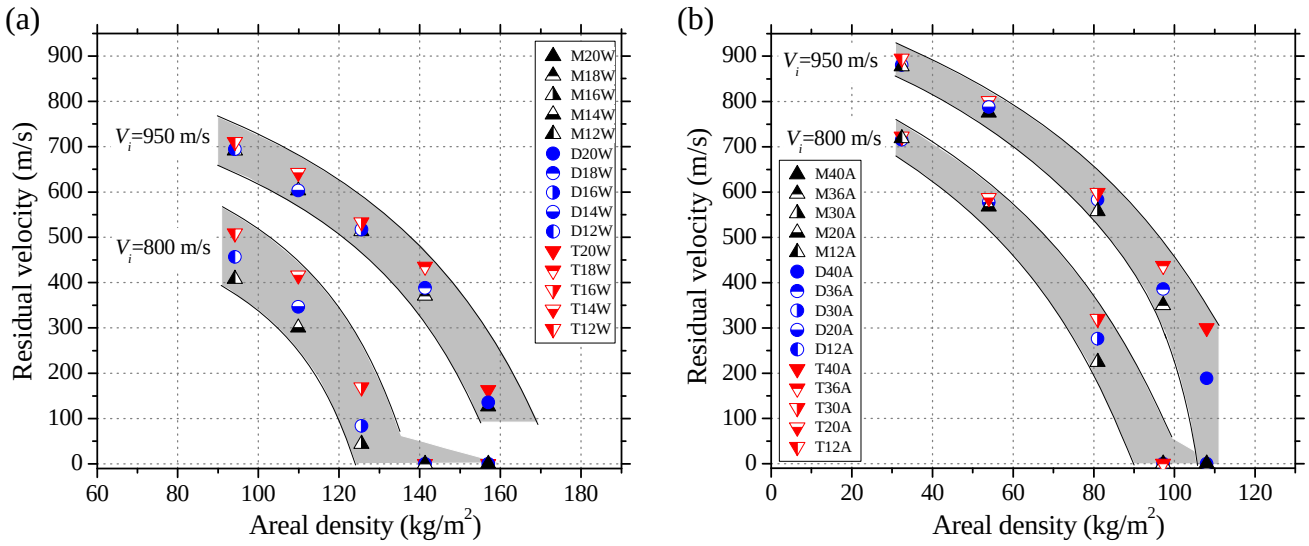

Figure 6 Residual velocity versus areal density for various multi-layered plate configurations of (a) Weldox 700E steel and (b) Al 7075-T651 plates for V_i=800 and 950 m/s.

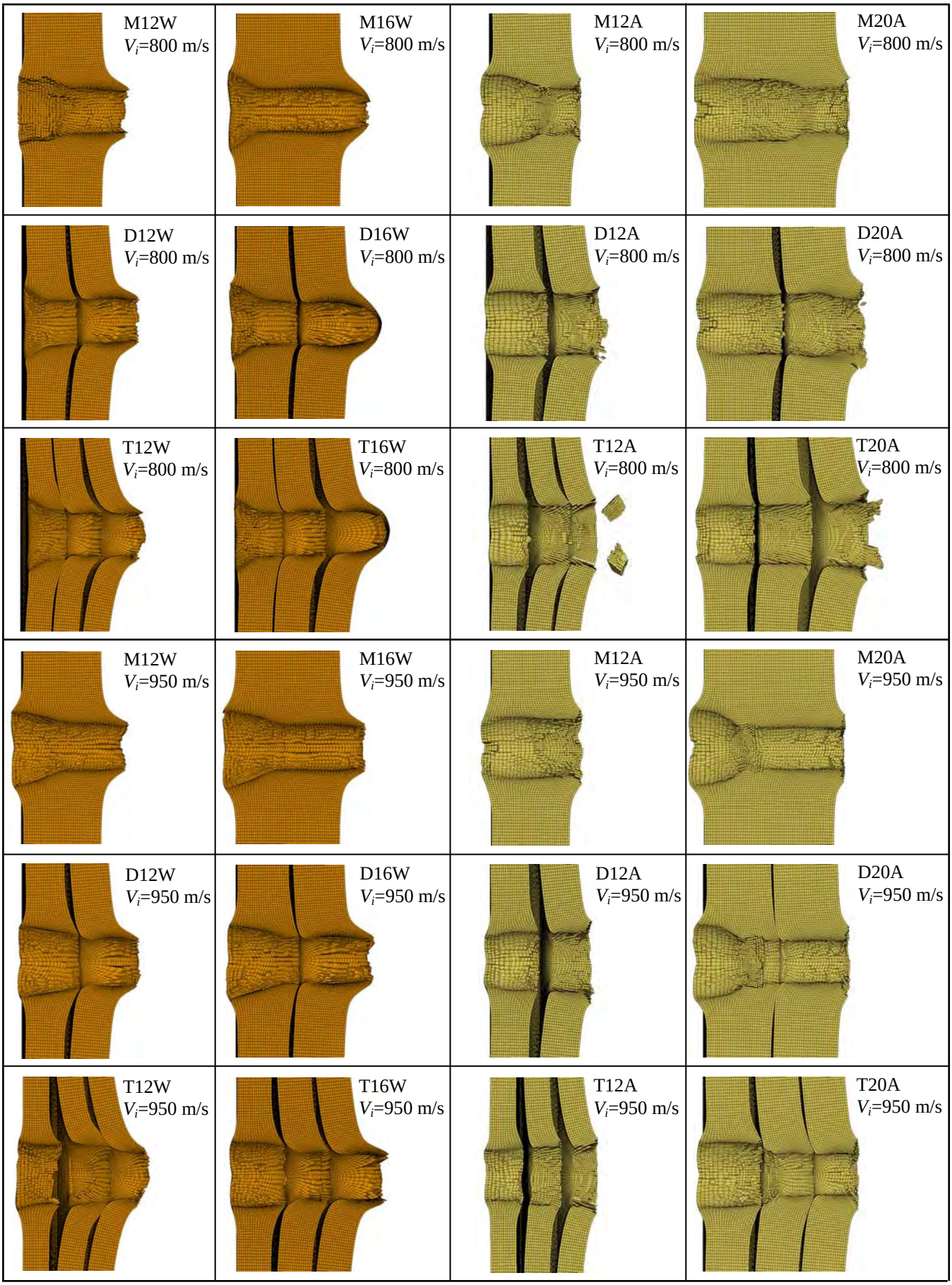

Figure 7 Penetration of M12W, D12W, T12W, M16W, D16W, T16W, M12A, D12A, T12A, M20A, D20A and T20A at t=0.07 ms, and initial velocities of V_i=800 and 950 m/s.

It can be seen in Fig. 6 that the ballistic performance of Al 7075-T651 is superior than that of Weldox 700E when compared for similar areal density, which is in agreement with reported experimental data [7, 12]. For example, for monolithic Weldox 700E plate at V_i≈800 m/s and ρ_A≈94 kg/m^2 (12 mm thickness), the residual velocity is V_r≈400 m/s (Fig. 5(a)), while for monolithic Al 7075-T651 plate at V_i≈800 m/s and ρ_A=81 kg/m^2 (30 mm thickness), the residual velocity is V_r≈230 m/s (Fig. 5(b)). However, when the ballistic performances are compared for similar thicknesses, Weldox 700E configurations perform better. Al 7075-T651 plates should be at least twice thicker than Weldox 700E plates to exhibit greater ballistic resistance, which could be a limiting factor for design purposes.

The indication that Al 7075-T651 exhibits better ballistic resistance than Weldox 700E for similar areal density raises an interesting question as to whether a multi-layered target made with a combination of steel and aluminium alloy may have a greater resistance than that of targets made only with steel of similar areal density. This question is addressed in the next Section by investigating multi-layered mixed targets with thickness equal to or less than 20 mm.

3.2 Effect of multi-layered mixed configuration

The effects of multi-layered mixed configurations on the ballistic performance were studied using double-layered mixed and triple-layered mixed plates with ρ_A=122.7 kg/m^2, made with a combination of Weldox 700E and Al 7075-T651. An initial impact velocity of 810 m/s was first used to observe the effectiveness of the targets, expressed by the residual velocity (Fig. 8). Results for steel plates (M16W, D16W, T16W, see Table 1) with similar areal density (ρ_A=125.7 kg/m^2) are also shown in Fig. 8 for comparison. It can be seen that the double-layered mixed configuration DM20AW has the best performance while triple-layered steel plates T16W has the poorest performance. To assess the performance of the different configurations, further numerical simulations were carried out for a wider range of velocities (775-950 m/s) for DM20AW, DM20WA, TM20AWW, M16W, D16W and T16W configurations (Fig. 9). The solid lines represent fits to the numerical data of the Retch-Ipson model (Eq. (4)) using at least six data points. The method of least squares was used to obtain the best fit of P and V_{bl} [28]; these values are shown in Table 3.

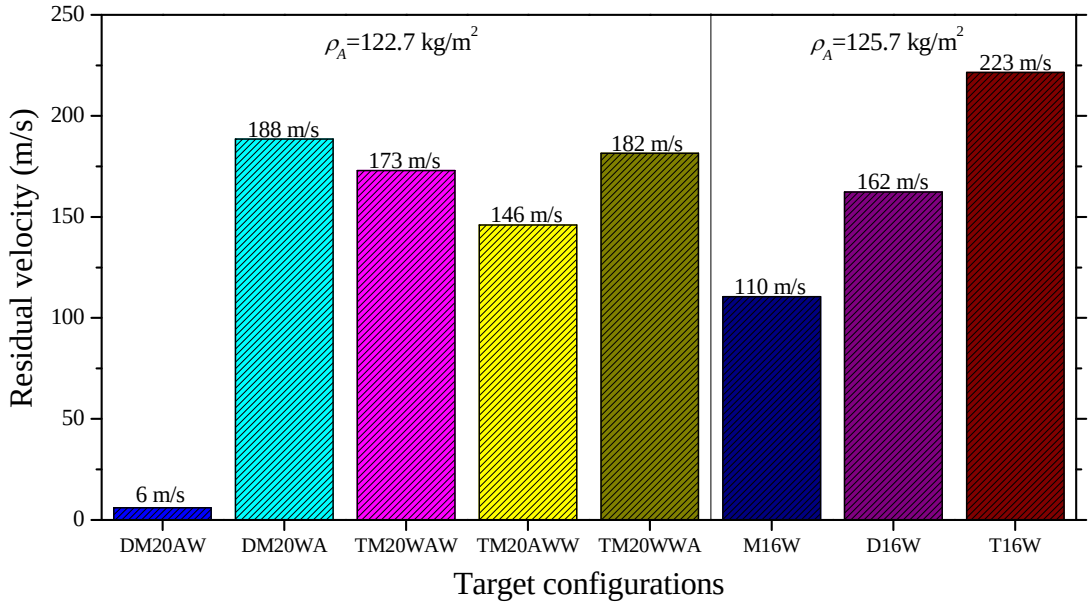

Figure 8 Residual velocity for various multi-layered mixed plates and Weldox 700E plate configurations for V_i=810 m/s.

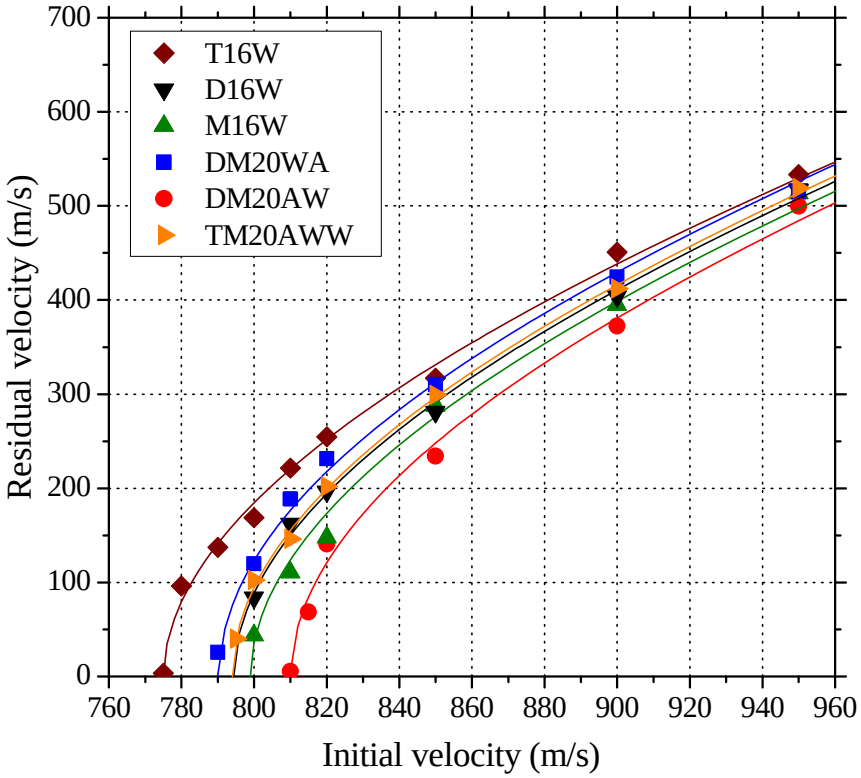

Figure 9 Residual velocity versus initial velocity for various multi-layered mixed and Weldox 700E configurations.

Table 3 Ballistic limit and Recht-Ipson parameters for various target configurations.

	DM20AW	DM20WA	TM20AWW	M16W	D16W	T16W
V_{bl} (m/s)	810.1	789.9	794	798.9	794.4	774.9
a	1	1	1	1	1	1
P	1.95	1.99	1.97	1.94	1.95	1.93

It can be seen in Fig. 9 that the trend of ballistic performances observed in Fig. 8 is observed for all impact velocities. Monolithic M16W and double-layered D16W show a similar ballistic resistance, which is in agreement with experimental results [7].

Figures 10 shows projectile velocity versus time for DM20AW, DM20WA, T16W, TM20AWW, D16W and M16W plates when impacted with an initial velocity of 820 m/s. Perforation of plates at t=0.04 and 0.07 ms is also depicted. It can be seen that the mechanisms involved in the penetration process are different for each case and they define the difference in the ballistic performance. At t=0.04 ms, V≈400 m/s for DM20AW and M16W, V≈450 m/s for DM20AW, T16W and D16W; and V≈500 m/s for TM20AWW. This variation is explained by the fact that there is a reduction of bending stiffness in T16W and TM20AWW, and less resistance to penetration in DM20AW and TM20AWW because the first layer (Al 7075-T651) has a lower strength than Weldox 700E. This effect can be observed in the reduction of the stripping of the brass jacket in DM20AW and TM20AWW when compared with the other configurations (Fig. 10 at t=0.04 ms). At t=0.07 ms, T16W plates exhibit the lowest performance when compared to DM20AW and DM20WA (Fig. 10a), which could be attributed to the greater bending resistance of the other two configurations.

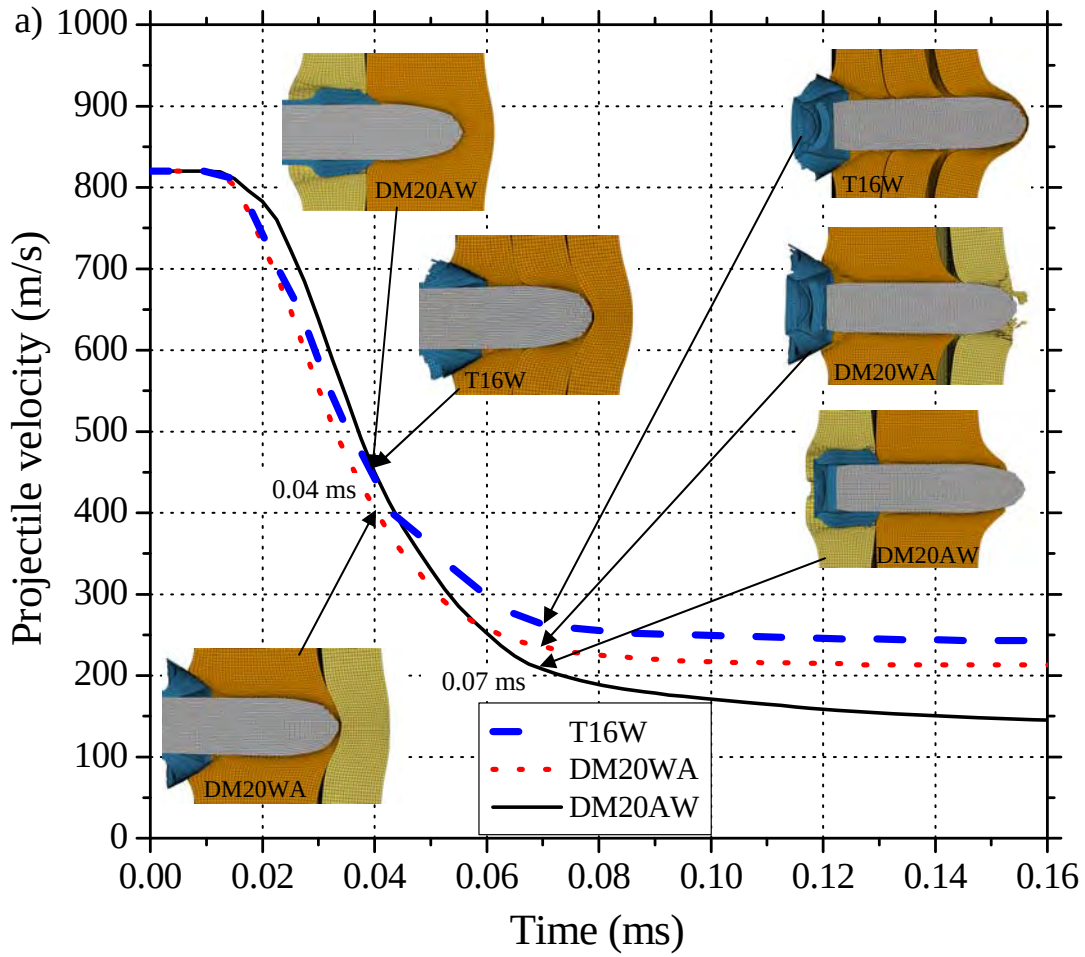

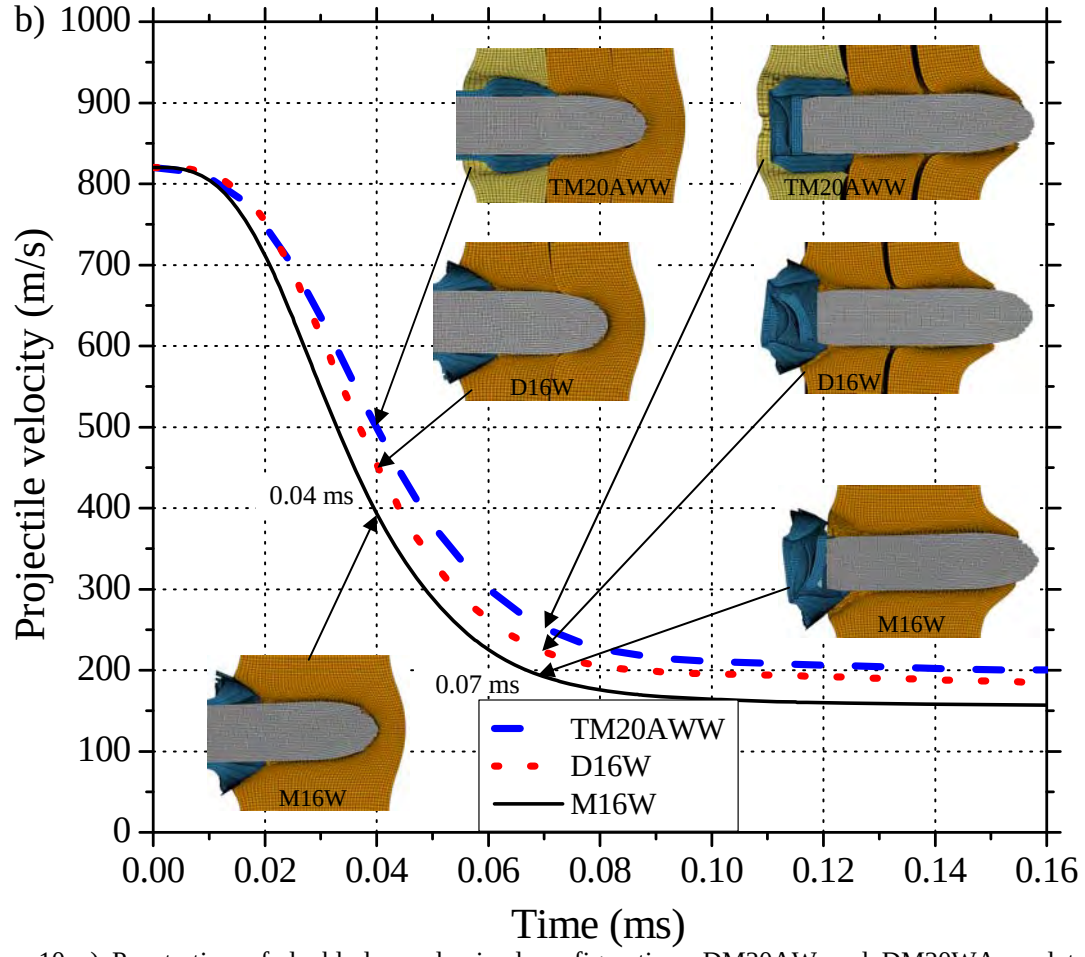

Figure 10 a) Penetration of double-layered mixed configurations DM20AW and DM20WA, and triple-layered configuration T16W for an initial impact velocity of 820 m/s; b) penetration of triple-layered mixed configuration TM20AWW, double-layered configuration D16W and monolithic configuration M16W for an initial impact velocity of 820 m/s.

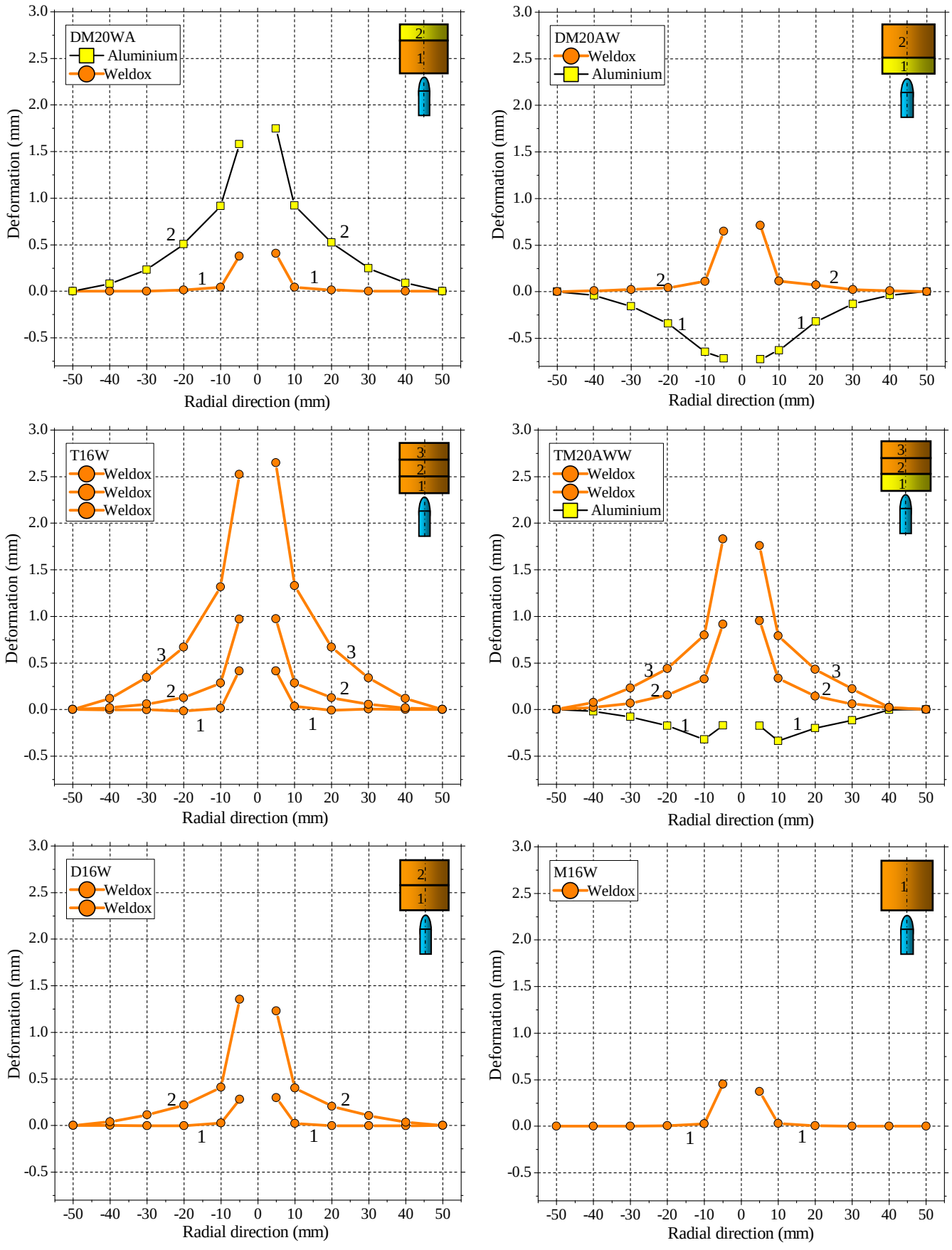

Figure 11 Permanent deformation profiles for target configurations shown in Fig. 10 and an initial impact velocity of 820 m/s.

It can be seen in Fig. 10b that M16W exhibits better performance than D16W and TM20AWW while the performance of D16W and TM20AWW is similar (Fig. 9). It is noticeable that the performance of DM20AW becomes greater than that of DM20WA at approximately t=0.06 ms (Fig. 10a). This performance can be explained by the fact that the Al 7075-T651 back plate of the DM20WA configuration fails by brittle fracture. Borvik et al. [11] reported this type of failure in 20 mm thick Al 7075-T651 plates when impacted by ogival projectiles. Brittle failure contrasts with the ductile failure of the steel back plate of DM20AW. It is believed that the front Al 7075-T651 plate of DM20AW does not fail by brittle fracture due to the backing support of the steel back plate. This behaviour is further illustrated in Fig. 11, where permanent deformation profiles for target configurations in Fig. 10 are shown. It can be seen in Fig. 11a and 11b that the back plate of DM20AW (Al 7075-T651) exhibits larger permanent deformation than the back plate of DM20AW. It can also be seen in Fig. 11 when comparing M16W, D16W and T16W that the permanent deformation increases with an increase in the number of layers.

4 SUMMARY AND CONCLUSIONS

A numerical investigation of the ballistic performance of monolithic and multi-layered targets made with either Weldox 700E steel or Al 7075-T651 or a combination of these materials against 7.62-mm APM2 projectiles was conducted, for the velocity range of 775-950 m/s and various target thicknesses. A corresponding experimental study would be prohibitively expensive and difficult. Numerical simulations demonstrated the capability of the model to predict the ballistic behaviour of Weldox 700E and Al 7075-T651, and reproduced many of the physical characteristics of the penetration process observed experimentally. The numerical model developed in this research could be used for the design of experimental testing by reducing the number of necessary tests and minimising necessary resources; however, it should be considered that the results obtained in this study are based on numerical simulations, and experimental validation should be performed.

For Weldox 700E, it was observed that monolithic plates perform better than triple-layered plates, which is more noticeable for an impact velocity of 800 m/s. The difference in performance between monolithic and double-layered plates was not significant. For Al 7075-T651, the difference in performance between monolithic and multi-layered plates is not significant for thicknesses less than 20 mm, while for thickness greater than 30 mm there is a large difference in performance. Further investigation (both experimental and numerical) should be performed to assess the validity of the numerical model for Al 7075-T651 at thicknesses greater than 30 mm.

Numerical and experimental results show that Al 7075-T651 has a better ballistic performance than Weldox 700E when compared for similar areal density; however, Al 7075-T651 plates have to be at least twice thicker than Weldox 700E plates to exhibit this superior performance, which could be limiting for design purposes. Multi-layered configurations made with a combination of steel and aluminium and a maximum thickness of 20 mm were also investigated. It was found that a double-layered mixed configuration with a front Al 7075-T651 plate and a Weldox 700E steel back plate (DM20AW) performs better than any other configuration with similar areal density. This finding shows that an armour shield made of two different materials may potentially perform better than the equivalent steel plate. However, the results in this study are limited and further research has to be carried out to fully understand this type of target configuration since there are few studies addressing this research topic [3].

It is concluded that multi-layered mixed plates made with a combination of high strength aluminium alloys and steels are an interesting option for protective structures because they may potentially lead to weight-savings and improvement of the ballistic performance of the structure.

However, further numerical and experimental research has to be carried out to support the findings in this study.

ACKNOWLEDGEMENTS

The authors would like to thank the Defence Materials Technology Centre (DMTC) for its financial support, which made this research possible. DMTC was established and is supported by the Australian Government's Defence Future Capability Technology Centre (DFCTC) initiative.

REFERENCES

[1] J.A. Zukas, D.R. Scheffler, Impact effects in multilayered plates, Int. J. Solids Struct., 38 (2001) 3321-3328.

[2] S. Dey, T. Børvik, X. Teng, T. Wierzbicki, O.S. Hopperstad, On the ballistic resistance of double-layered steel plates: An experimental and numerical investigation, Int. J. Solids Struct., 44 (2007) 6701-6723.

[3] X. Teng, T. Wierzbicki, M. Huang, Ballistic resistance of double-layered armor plates, Int. J. Impact Eng., 35 (2008) 870-884.

[4] D.W. Zhou, W.J. Stronge, Ballistic limit for oblique impact of thin sandwich panels and spaced plates, Int. J. Impact Eng., 35 (2008) 1339-1354.

[5] A.A. Almohandes, M.S. Abdel-Kader, A.M. Eleiche, Experimental investigation of the ballistic resistance of steel-fiberglass reinforced polyester laminated plates, Compos. Part B, 27 (1996) 447-458.

[6] N.K. Gupta, V. Madhu, An experimental study of normal and oblique impact of hard-core projectile on single and layered plates, Int. J. Impact Eng., 19 (1997) 395-414.

[7] T. Børvik, S. Dey, A.H. Clausen, Perforation resistance of five different high-strength steel plates subjected to small-arms projectiles, Int. J. Impact Eng., 36 (2009) 948-964.

[8] X. Teng, S. Dey, T. Børvik, T. Wierzbicki, Protection performance of double-layered metal shields against projectile impact, J. Mech. Mater. Struc., 2 (2007) 1309-1329.

[9] R.S.J. Corran, P.J. Shadbolt, C. Ruiz, Impact loading of plates -- An experimental investigation, Int. J. Impact Eng., 1 (1983) 3-22.

[10] K.O. Pedersen, T. Børvik, O.S. Hopperstad, Fracture mechanisms of aluminium alloy AA7075-T651 under various loading conditions, Mater. Des., 32 (2011) 97-107.

[11] T. Børvik, O.S. Hopperstad, K.O. Pedersen, Quasi-brittle fracture during structural impact of AA7075-T651 aluminium plates, Int. J. Impact Eng., 37 (2010) 537-551.

[12] M. Forrestal, T. Børvik, T. Warren, Perforation of 7075-T651 aluminum armor plates with 7.62 mm APM2 bullets, Exp. Mech., 50 (2010) 1245-1251.

[13] P.K. Jena, B. Mishra, K. Siva Kumar, T.B. Bhat, An experimental study on the ballistic impact behavior of some metallic armour materials against 7.62 mm deformable projectile, Mater. Des., 31 (2010) 3308-3316.

[14] P.K. Jena, K. Ramanjeneyulu, K. Siva Kumar, T. Balakrishna Bhat, Ballistic studies on layered structures, Mater. Des., 30 (2009) 1922-1929.

[15] J.O. Hallquist, LS-DYNA Keyword User's Manual, Version 971, Livermore Software Technology Corporation, California, (2007).

[16] NATO STANAG 4569 Ed. 1; Protection levels for occupants of logistic and light armoured vehicles, (2004).

[17] M. Saleh, L. Edwards, Evaluation of a hydrocode in modelling NATO threats against steel armour, in: 25th International Symposium on Ballistics, Beijing, China, 2010.

[18] T. Børvik, O.S. Hopperstad, T. Berstad, M. Langseth, A computational model of viscoplasticity and ductile damage for impact and penetration, Eur. J. Mech. A-Solid, 20 (2001) 685-712.
[19] G.R. Johnson, W.H. Cook, A constitutive model and data for metals subjected to large strains, high strain rates and high temperatures, in: Proceedings of the 7th International Symposium on Ballistics, The Hague, The Netherlands, 1983.
[20] M.G. Cockcroft, D.J. Latham, Ductility and the workability of metals, J. Inst. Metals, 96 (1968) 33-39.
[21] T. Børvik, S. Dey, O.S. Hopperstad, M. Langseth, On the main mechanisms in ballistic perforation of steel plates at sub-ordnance impact velocities, in: S. Hiermaier (Ed.) Predictive modeling of dynamic processes, Springer, Dordrecht, 2009, pp. 189-219.
[22] A. Kane, T. Borvik, O.S. Hopperstad, M. Langseth, Finite element analysis of plugging failure in steel plates struck by blunt projectiles, J. Appl. Mech., 76 (2009) 051302-051311.
[23] T. Børvik, M.J. Forrestal, O.S. Hopperstad, T.L. Warren, M. Langseth, Perforation of AA5083-H116 aluminium plates with conical-nose steel projectiles - Calculations, Int. J. Impact Eng., 36 (2009) 426-437.
[24] E. Fagerholt, F. Grytten, B.E. Gihleengen, M. Langseth, T. Børvik, Continuous out-of-plane deformation measurements of AA5083-H116 plates subjected to low-velocity impact loading, Int. J. Mech. Sci., 52 (2010) 689-705.
[25] F. Grytten, T. Børvik, O.S. Hopperstad, M. Langseth, Low velocity perforation of AA5083-H116 aluminium plates, Int. J. Impact Eng., 36 (2009) 597-610.
[26] R.F. Recht, T.W. Ipson, Ballistic perforation dynamics, J. Appl. Mech., 30 (1963) 384-390.
[27] T. Ipson, R. Recht, Ballistic-penetration resistance and its measurement, Exp. Mech., 15 (1975) 249-257.
[28] T. Børvik, O.S. Hopperstad, M. Langseth, K.A. Malo, Effect of target thickness in blunt projectile penetration of Weldox 460 E steel plates, Int. J. Impact Eng., 28 (2003) 413-464.